frontiers in Marine Science

MINI REVIEW
published: 22 July 2021
doi: 10.3389/fmars.2021.676537

Radiometry on Argo Floats: From the Multispectral State-of-the-Art on the Step to Hyperspectral Technology

Ahlem Jemai[1], Jochen Wollschläger[1], Daniela Voß[1] and Oliver Zielinski[1,2]*

[1] Center for Marine Sensors (ZfMarS), Institute for Chemistry and Biology of the Marine Environment (ICBM), Carl von Ossietzky University Oldenburg, Wilhelmshaven, Germany, [2] Marine Perception Research Department, German Research Center for Artificial Intelligence (DFKI), Oldenburg, Germany

Over the past two decades, robotic technology such as Argo floats have revolutionized operational autonomous measurement of the oceans. Recently, Biogeochemical Argo floats (BGC-Argo floats) have measured optical and biogeochemical quantities down to a depth of 2,000 m. Among these parameters, are measurements of the underwater light field from which apparent optical properties (AOPs), such as the diffuse attenuation coefficient for downwelling irradiance $K_d(\lambda)$, can be derived. Presently, multispectral observations are available on this platform at three wavelengths (with 10–20 nm bandwidths) in the ultraviolet and visible part of the spectrum plus the Photosynthetically Available Radiation (*PAR*; integrated radiation between 400 and 700 nm). This article reviews studies dealing with these radiometric observations and presents the current state-of-the-art in Argo radiometry. It focus on the successful portability of radiometers onboard Argo float platforms and covers applications of the obtained data for bio-optical modeling and ocean color remote sensing. Generating already high-quality datasets in the existing configuration, the BGC-Argo program must now investigate the potential to incorporate hyperspectral technology. The possibility to acquire hyperspectral information and the subsequent development of new algorithms that exploit these data will open new opportunities for bio-optical long-term studies of global ocean processes, but also present new challenges to handle and process increased amounts of data.

Keywords: radiometry, Argo floats, underwater light field, apparent optical properties, ocean sensing

OPEN ACCESS

Edited by:
Fei Chai,
Second Institute of Oceanography, Ministry of Natural Resources, China

Reviewed by:
Xiaogang Xing,
Second Institute of Oceanography, Ministry of Natural Resources, China
Emanuele Organelli,
National Research Council (CNR), Italy

****Correspondence:***
Ahlem Jemai
Ahlem.jemai@uni-oldenburg.de

Specialty section:
This article was submitted to Ocean Observation, a section of the journal Frontiers in Marine Science

Received: *05 March 2021*
Accepted: *25 June 2021*
Published: *22 July 2021*

Citation:
Jemai A, Wollschläger J, Voß D and Zielinski O (2021) Radiometry on Argo Floats: From the Multispectral State-of-the-Art on the Step to Hyperspectral Technology. Front. Mar. Sci. 8:676537. doi: 10.3389/fmars.2021.676537

INTRODUCTION

The marine environment is highly complex, and conventional *in situ* measurements carried out, e.g., on research cruises, can only provide a series of snapshots. Therefore, uncovering the real dynamics requires complementation with data of higher spatiotemporal coverage, which could be provided by autonomous measurements (Zielinski et al., 2009; Chai et al., 2020). The Argo network of autonomous floats[1] has revolutionized the capability for operational observations (Roemmich, 2001) to be the main source of CTD measurements (Riser et al., 2016). Biogeochemical Argo floats (BGC-Argo floats) (Biogeochemical-Argo Planning Group, 2016), the extension of the Argo core mission, supply the optical and biogeochemical observations necessary to construct a

[1]https://argo.ucsd.edu

global, full-depth, and multidisciplinary ocean-observing system (IOCCG, 2011; Bittig et al., 2019; Claustre et al., 2020). This type of float accommodates up to six essential biogeochemical and bio-optical variables (**Figure 1**): oxygen (O_2), pH, nitrate (NO_3), suspended particles, chlorophyll-a (chl-a), and radiometry.

The basic radiometric measurement is the spectral radiance, $L(\lambda)$, representing the radiant flux from a defined direction through a defined area. From radiance, all other integral measures of the light field can be derived, such as irradiance $E(\lambda)$,which is the total radiant flux per unit area of horizontal surface measured in the direction of the incoming light. The downwelling irradiance $E_d(\lambda)$, thus the irradiance measured toward the sea surface, is the parameter that is regularly measured by the BGC-Argo floats (Organelli et al., 2016). However, some initiatives have started to look also at the upwelling radiance L_u (Gerbi et al., 2016; Leymarie et al., 2018; Wojtasiewicz et al., 2018). The propagation of $E_d(\lambda)$ in the water column can be described approximately as an exponential function of depth (Mobley, 1994):

$$E_d(\lambda, z) = E_d\left(\lambda, 0^-\right) e^{\int_z^0 -K_d(\lambda,z).dz} \quad (1)$$

In case a layer-averaged K_d (from 0 to z) is used, light decline is calculated according to:

$$E_d(\lambda, z) = E_d\left(\lambda, 0^-\right) e^{-K_d(\lambda,z).z} \quad (2)$$

There, z [m] is water depth, $E_d\left(\lambda, 0^-\right)$ [$Wm^{-2}sr^{-1}nm^{-1}$] the irradiance right below the surface, and $K_d(\lambda, z)$ [m^{-1}] the diffuse attenuation coefficient of downwelling irradiance, which can be deduced from measurements of E_d in different depths. Both E_d and K_d are spectral quantities, indicated by λ [nm] for wavelength.

The slope of this exponential decline, thus $K_d(\lambda)$, depends on the absorption (a)and backscattering properties (b_b) of the water (Lee et al., 2005), i.e., termed the inherent optical properties (IOPs), which are in turn determined by the water molecules themselves as well as the properties and concentration optically active substances (OAS) within the water column, such as phytoplankton, detrital matter, and colored dissolved organic matter (CDOM; see also Kirk, 2011). From $E_d(\lambda)$ and $L_u(\lambda)$, other quantities, commonly known as apparent optical properties (AOPs), can be derived. In addition to $K_d(\lambda)$, a frequently derived AOP is radiance reflectance,$r_{rs}(\lambda)$, (or remote sensing reflectance, $R_{rs}(\lambda)$, when measured just above the sea surface). It is defined as the ratio of $L_u(\lambda)/E_d(\lambda)$ (see Morel and Gentili, 1996). A multiplication with the extraterrestrial solar spectral irradiance, gives another important parameter, the normalized water-leaving radiance, $L_{wn}(\lambda)$ (see Gordon and Clark, 1981). $K_d(\lambda)$, $r_{rs}(\lambda)$, and $R_{rs}(\lambda)$ are also the most commonly studied parameters of interest in remote sensing applications, notably satellite observation (Austin and Petzold, 1981; Werdell and Bailey, 2005). However, converting a radiometric signal captured by a spaceborne sensor to an end-user product carries uncertainties. High demands for accuracy in absolute calibration of satellite remote sensing data (IOCCG, 2013) and high quality field observations are required for satellite product validation/evaluation (Mueller and Austin, 1992; Zibordi and Voss, 2014). For both optical *in situ* and remote sensing observation, various bio-optical algorithms have been developed to relate features of the water signal to in-water quantities of interest (e.g., O'Reilly et al., 1998; Maritorena et al., 2002). Improving these retrieval algorithms (existing) and develop enhanced ones that exploit forthcoming technologies remains a priority for ocean optics community.

Ocean optics research has recently undergone a shift from multispectral (with broadband data) to hyperspectral instrumentation, both *in situ* and remotely (Chang et al., 2004). The higher number of available bands in hyperspectral observations allows a more detailed examination regarding spectral resolution of AOPs and IOPs within the water column. This makes applications requiring higher resolution feasible, e.g., the discrimination of phytoplankton groups, the determination of particle size, and more detailed determination of CDOM spectral properties. Conventional Argo floats already provide sustained high-quality data at unprecedented temporal and spatial resolution. Thus, the addition of hyperspectral observation capabilities will allow Argo platforms to meet demands regarding more sophisticated approaches from the field of optical models and remote sensing. The exploitation of such high-resolution data (in the spatial, temporal, and spectral dimension), measured by a single system that carries also IOP sensors, will certainly open new avenues for bio-optical research in the future. This exciting combination (Argo platform + hyperspectral radiometers) could be the next logical step for Argo floats network (Claustre et al., 2020). With this in mind, this review summarizes the current state-of-the-art of radiometric measurements on Argo floats, and identifies emerging future pathways for the development of hyperspectral Argo radiometry and data exploitation. In our search, we referred to the list of the BGC Argo mission bibliography,[2] from which we selected studies involving radiometric measurements (including papers describing data management approaches and quality-control procedures). We made additional research using Google Scholar and Scopus for verification.

ARGO-RADIOMETRY: STATE-OF-THE-ART

Instrumentation

The radiometer mounted on BGC-Argo floats at the time of this review is the multispectral Ocean Color Radiometer (OCR-504, SATLANTIC Inc./Sea-Bird Scientific, United States) (SATLANTIC, 2013), which measures irradiance commonly at four channels. Three channels are usually dedicated to narrow-wavelengths (around 10 or 20 nm bandwidth) from the ultraviolet to the visible range of the spectrum, while the fourth channel measures the Photosynthetically Available Radiation (*PAR*; integrated radiation between 400 and 700 nm). Two different sets of waveband configurations have been documented in the literature. Depending on the funding program, the earlier studies have applicated 412, 490, and 555 nm (Xing et al., 2011, 2012, 2014; Mignot et al., 2014). Later studies have selected

[2]https://argo.ucsd.edu/outreach/publications/biogeochemical-argo-bibliography

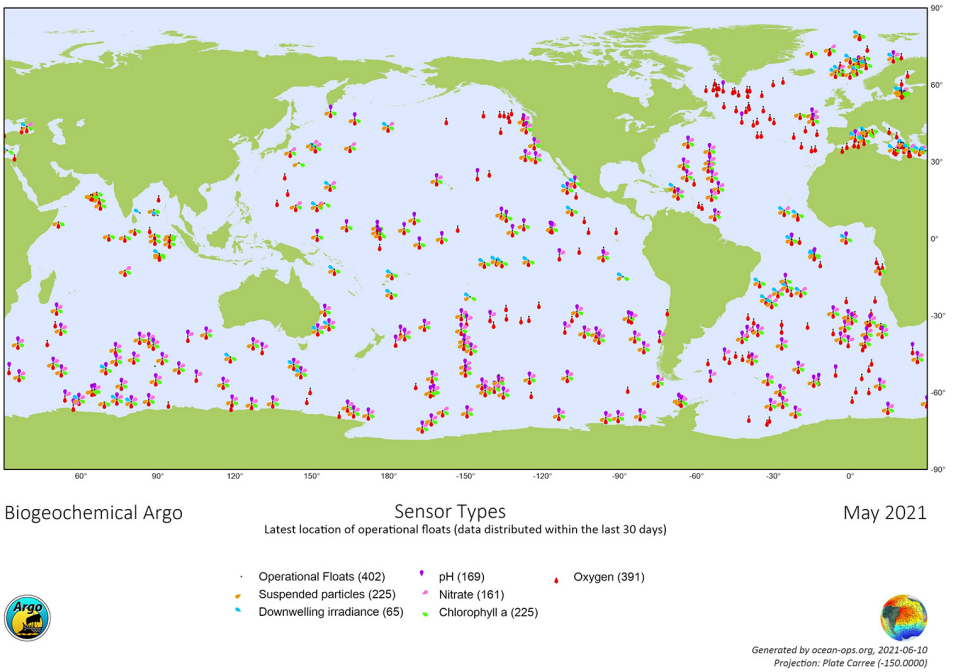

FIGURE 1 | Map depicting active floats and their equipped sensors (color classification), as of May 2021. For updated maps see the Biogeochemical-Argo website. Up to 40548 downwelling irradiance profiles have been acquired as of May 2021 (for an updated summary, see the Bio-geochemical-Argo website https://biogeochemical-argo.org/cloud/document/implementation-status/BGC_summary.pdf).

380 nm instead of 555 nm (Organelli et al., 2016; Organelli et al., 2017a,b; Mignot et al., 2018; Organelli and Claustre, 2019). The fourth channel dedicated to PAR was used in the context of determining overall light available for primary production in the ocean (Lacour et al., 2017, 2019; Mignot et al., 2018; Barbieux et al., 2019; Terzić et al., 2019). However, studies that measured both E_d and L_u have used the four wavelengths centered at 412, 443, 488, and 555 nm (Gerbi et al., 2016; Wojtasiewicz et al., 2018), and up to 7 wavelengths plus *PAR* using OCR507 (see Leymarie et al., 2018). **Table 1** summarizes available studies that made use of radiometric data obtained with Argo floats, with the exception of studies that exploit the data only as additional or support information. We also excluded studies that covered primarily data management or quality control protocols.

Exploitation of the Radiometric Data Obtained From Argo

The mapping of phytoplankton is an area of environmental monitoring that has particularly benefitted from the Argo radiometric observations. Indeed, the *PAR* observations acquired in high sampling frequency provide a comprehensive picture of the vertical distribution of phytoplankton chlorophyll over the different layers in the euphotic zone (surface layer, mixed layer, and deep chlorophyll maximum layer) (Mignot et al., 2014; Lacour et al., 2017, 2019; Barbieux et al., 2019; Ricour et al., 2021). Gaining such dynamic illustration of the light gradient, including the critical depth of the upper euphotic mixed layer, revealed the magnitude and timing of blooms occurring in otherwise inaccessible locations in different seasons (Randelhoff et al., 2020). However, with respect to phytoplankton diversity, these ecological events are still in demand for a monitoring in terms of pigment groups or functional types (Kutser, 2009), for which multispectral data provide not enough spectral resolution. Readily, this dataset has demonstrated also its utility in improving numerical biogeochemical modeling (Terzić et al., 2019). Other reviewed studies provided that *PAR* and/or *Ed* have also successfully used to validate IOP parameterizations (Lazzari et al., 2021). Biogeochemical quantities like chl-a and CDOM were also retrieved from $K_d(490)$ and $K_d(412)$, respectively (Xing et al., 2011, 2012), and other related studies disclosed their main drivers (Organelli and Claustre, 2019). The estimations of such biogeochemical quantities are still in need to be refined and improved better resolved with respect to their relative contribution to the in-water optical properties via their absorption and scattering signatures (Claustre et al., 2020). Acquiring radiometric data over the entire spectrum will permit the construction of continuous spectral diffuse attenuation information that, in turn, enables for depth-dependent IOPs characteristics of the OAS in the water column. Such analysis would be rather difficult with the fewer bands of a multispectral sensor (Chang et al., 2004).

Argo radiometric data plays further a significant role in increasing the amount of data available for satellite matchups in remote areas (Organelli et al., 2017a; Wojtasiewicz et al., 2018), as well as for evaluating the performance of ocean color remote sensing retrievals (Organelli et al., 2017a; Xing et al., 2020). Thus, a further exploitation of the Argo platform capabilities is

TABLE 1 | Summary of studies that used Argo radiometric data for their main research aim.

Type of Argo float	Optical quantity	Derived AOPs	Area studied	Aim	Author
Not specified	*PAR*		Black Sea	Vertical distribution of chlorophyll concentration	Ricour et al., 2021
Prolce	E_d (380, 412, 490) + *PAR*		Arctic	Study the phytoplankton growth	Randelhoff et al., 2020
Not specified	E_d (380, 412, 490) + *PAR*		Mediterranean Sea	Validation of numerical model of radiative transfer	Lazzari et al., 2021
Not specified	E_d (380, 412, 490) + *PAR*	K_d (*PAR*); K_d (490)	World's ocean (Southern Ocean, Subpolar Gyre, Transition zone, Red Sea, Black Sea, Mediterranean Sea, Subtropical Gyre, Arctic Sea, New Caledonia)	Evaluation of ocean color remote sensing algorithms for diffuse attenuation and optical depths	Xing et al., 2020
PROVOR (NKE Marine Electronics Inc., France)	E_d (380, 412, 490) + *PAR*	K_d (380); K_{bio} (380); K_{star} (380); K_d (490); K_{bio} (490)); K_{star} (490)	North Atlantic subtropical gyre	Understand the potential driver of CDOM	Organelli and Claustre, 2019
Not specified	*PAR*	K_d (*PAR*)	Mediterranean Sea	Improve the simulation of chl-a dynamics	Terzić et al., 2019
PROVOR (NKE Marine Electronics Inc., France)	*PAR*	Euphotic depth (Zeu)	North Atlantic subpolar Ocean	Light penetration information	Lacour et al., 2017, 2019
Navis (Sea-Bird Scientific, Inc., United States)	E_d (412, 443, 490, 555) L_u (412, 443, 490, 555)	R_{rs} (412, 443, 490, 555)	Indian Ocean subtropical gyres	Validation of remote sensing reflectance	Wojtasiewicz et al., 2018
PROVOR (NKE Marine Electronics Inc., France)	E_d (380, 443, 490, 510, 560, 665) + *PAR* L_u (380, 443, 490, 510, 560, 665) E_d (412, 443, 490, 510, 560, 665) + *PAR* L_u (380, 443, 490, 510, 560, 665)		Mediterranean Sea Southern Ocean	Test the applicability of the new PROVOR float (CTS5) in ocean color validation activities	Leymarie et al., 2018
Not specified	*PAR*	K_d (*PAR*)	North Atlantic subpolar Ocean	Determine the euphotic layer depth	Mignot et al., 2018
PROVOR CTS-4 (NKE Marine Electronics Inc., France)	E_d (380, 412, 490)+ *PAR*	K_d (380); K_d (490)	Black Sea; Subtropical gyres (Atlantic and Pacific); High latitudes (North Atlantic and southern oceans); Mediterranean Sea	Reexamine the regional variability of relationship between CDOM and phytoplankton light absorption properties referring to existing bio-optical models	Organelli et al., 2017b
APEX (Teledyne Webb Research., United States)	E_d (412, 443, 488, 555) L_u (412, 443, 488, 555)	R_{rs} (412, 443, 488, 555)	Mediterranean Sea; Pacific Ocean; Atlantic Ocean	Validation of remote sensing reflectance	Gerbi et al., 2016
PROVOR (NKE Marine Electronics Inc., France)	E_d (412, 490, 555)	K_d (412); K_{bio} (412)); K_{bio} (490)	Mediterranean Sea; North Atlantic; North Pacific gyre	Quantification of biogeochemical quantities	Xing et al., 2011, 2012

reasonable to enhance the utilization of satellite data in terms of product retrievals (with less uncertainties). A frequent requested product in this respect are e.g., the phytoplankton accessory pigments in order to characterize phytoplankton dynamics in more detail instead just in terms of biomass (Mueller and Fargion, 2002). Other reviewed papers here have implicated the radiometric Argo data as a metric to get supplementary information about the euphotic zone and optical depth (Doxaran et al., 2014; Mayot et al., 2017), and to resolve events undetectable by satellite observations or classical sampling, for example, variation in optical depth preceding and following a typhoon event (Doxaran et al., 2014).

Other gains sum up in inclusion this dataset in those procedures of fluorometer (accompanied sensor on Argo float) calibration. For instance, measurement of $E_d(490)$ enables the retrieval of a scaling factor required for the calibration of the chl-a fluorometers (Xing et al., 2011). The reliability of this method was supported by later works (Xing et al., 2012, 2014; Mignot et al., 2014; Ardyna et al., 2019; Kubryakov et al., 2019). Argo *PAR* profiles have been also used to ameliorate the non-photochemical quenching (NPQ) correction of Argo chl-a fluorescence measurements (Xing et al., 2018).

Data Availability and Quality Control

As with all BGC-Argo variables, radiometric datasets are available within 24 h of transmission to the public in the Argo Global Data Assembly Centers (GDACs) along with the corresponding CTD data (Wong et al., 2020). The international Argo Data Management Team (ADMT) supervises the development of data management procedures of Argo data (Argo Data Management Team, 2021). As expected, this review observed a regular protocol in the way of acquiring and processing radiometric data (Schmechtig et al., 2017). In terms of quality control, two levels are generally applied: the "real time mode" that effectuates quick automatic checks (e.g., global range test) to ensure data provision to the user in near real time (Poteau et al., 2019); and the "delayed mode" based on scientific judgement, to account for confounding effects such as biofouling and sensor drift (Schmid et al., 2007), as well as other sources of uncertainty, e.g., the temperature effect on dark counts (Organelli et al., 2017a; Wojtasiewicz et al., 2018). In the earliest stage of the BGC-Argo program, Xing et al. (2011) relied on interpreting the chl-a fluorescence profiles that accompanied the downwelling irradiance measurements to obtain noise-free radiometric profiles. Later, Organelli et al. (2016) developed a quality-control procedure based on statistical and mathematical analyses that targets the major issues related to vertical in-water light field measurements (e.g., dark signal, clouds, wave-focusing, general spike detection; see also Mueller et al., 2003), taking into account the specific circumstances of the Argo platform (e.g., lack of operator control and float recovery precluding post-deployment check or recalibration of the radiometer). As no above-water measurements are available to validate the subsurface radiometric measurement, the comparison of the near-surface measurements with the output of clear-sky optical models (Gregg and Carder, 1990) was suggested to evaluate the obtained measurements (Xing et al., 2011; Organelli et al., 2016).

FUTURE PROSPECTS

Argo radiometric measurements are currently limited to observations measuring, depending on configuration, either irradiance or radiance at up to four channels. Acquisition of radiometric observations takes place in discrete spectral bands, selected to detect major variations in underwater optical properties, allowing these multispectral devices to be effective in deriving the relative concentration of in-water constituents over the water column. Taking the example of phytoplankton, the retrieval of more details regarding species composition (which is oftentimes called for) has been challenging because of the insufficient spectral resolution of the multispectral sensor (Bracher et al., 2017). Hyperspectral radiometers successfully achieved this discrimination (e.g., Isada et al., 2015; Xi et al., 2015), as well as the retrieval of phytoplankton functional types (Wolanin et al., 2016), as they provide measurements at hundreds of contiguous wavebands distributed equally from the ultraviolet to the near-infrared segment of the spectrum with a resolution of the order of 5 nm. This has led to more frequent use of hyperspectral instrumentation in ocean optics research (Chang et al., 2004). Bringing hyperspectral devices into play on robotic platforms such as Argo floats is therefore the next logical step (Claustre et al., 2020). In some, especially remote areas affected by regularly occurring (harmful) algal blooms, monitoring strategies require increased observing capabilities (Sellner et al., 2003). Whilst detection and characterization of the spatial and temporal development of phytoplankton biomass is already feasible using existing multispectral Argo floats, the transformation toward hyperspectral technology will provide additional opportunities of tracking its composition and predict harmful algal bloom development (Shen et al., 2012; Dierssen et al., 2020). Ultimately, hyperspectral data based on Argo float may pave the way toward harmful algal bloom forecasting programs that require nearly real time observations from a global communication network (Jochens et al., 2010).

Hyperspectral data is further advantageous for calibration and validation purposes (McClain and Meister, 2012) of current and future hyperspectral ocean color missions such as the Environmental Mapping and Analysis Program (EnMAP) (Guanter et al., 2015), the Hyperspectral Precursor of the Application Mission (PRISMA) (Loizzo et al., 2018), and the Pre-Aerosol, Clouds, and ocean Ecosystem (PACE) mission (Gregg and Rousseaux, 2017). Indeed, hyperspectral radiometric observations measured by Argo will provide high-resolution data (in the context of spatial, temporal and spectral resolution) that will be more appropriate to match the spectral bands of these advanced sensors (Werdell et al., 2013; Brewin et al., 2016). This would subsequently improve the assessment of derived products and thereby upgrade the validation metrics (Maritorena and Siegel, 2005; Maritorena et al., 2010; Seegers et al., 2018). A particular benefits of such datasets would be that they offer the possibility to develop new algorithms with more freedom in selecting spectral bands for bio-optical studies. Such developments would in turn improve both empirical remote-sensing (Gordon and Morel, 1983; Lee et al., 1998; Stramska et al., 2003) and semi-analytical approaches

(Carder et al., 1999), including the evaluation of radiative transfer modeling simulations (Mobley and Sundman, 2008). This would also serve as a contribution to the tuning of existing (heritage) IOP retrieval approaches (Werdell et al., 2018).

Hyperspectral Argo data, on other hand, will have their own scientific value in lieu of just supporting satellite missions. The exploitation of high-resolution data (in the spatial, temporal, and spectral extension), measured by a single system that carries also IOP sensors, would potentially reduce uncertainties (due to temporal or spatial biases) in existing inverse algorithms (Rehm and McCormick, 2011). Thence, the availability of hyperspectral AOPs quantities will enable the derivation of high spectral resolution IOP data, and this will considerably reduce the ambiguities introduced by the relative contribution of different accessory phytoplankton pigments for example, as well as retrieving CDOM spectral optical properties which bring additional biogeochemical information (Gordon et al., 2009). The investigation of such contemporaneous measurements is demonstrated in the work of Rehm and Mobley (2013) where they estimated absorption and backscattering coefficients to an accuracy of ± 0.01 m^{-1} and ± 0.0005 m^{-1} respectively, based on hyperspectral vertical radiometric observations and concurrent measurements of the beam attenuation coefficient at 650 nm in optically simple oligotrophic waters. In the more optically complex waters where OAS do not covary with chl-a, Wollschläger et al. (2020) obtained a moderately complex parametrization of the underwater light field based on hyperspectral light measurements. Such parametrizations could be strongly improved by accounting for seasonal and regional variation based on data coming from hyperspectral Argo-floats. Increasing the number of bands will moreover allow testing of various wavelengths combinations based on the spectral diffuse attenuation to better link IOPs features (Brown et al., 2004), as well as to check for consistency of calibration of fluorescence observations (accompanied sensor on Argo float) (Xing et al., 2011).

The deployment of hyperspectral radiometers on unattended platforms like Argo floats applies higher demands on the capabilities of the sensors than conventional in-water radiometry. Some studies which performed hyperspectral light field measurements using drifting devices (Zielinski et al., 2006; Barnard et al., 2018) have already demonstrated stable short-term field deployment of autonomous hyperspectral radiance and irradiance measurements. However, both studies highlight the importance of technical features like radiometer power consumption, long-term stability and reliability, standardized interfaces and protocols, as well as intelligent data handling. At present, the first studies are performed to evaluate the use of hyperspectral radiometers on Argo floats. The sensor used for these studies is an improved, 1,000 m-depth rated RAMSES radiometer (TRIOS, Rastede, Germany) designed to collect the incoming irradiance in the spectral range of 320–950 nm, with a spectral resolution of 2.2 nm and a spectral accuracy of 0.2 nm. The sensor also features the new G2 Modbus-interface for easier platform integration (Trios, 2021). An important consideration for Argo-users is that the increased information content increases the demand for data transfer and processing capabilities. Handling huge amounts of data within a timeframe of 24 h as strived by the Argo community will be a demanding task. In case of the mentioned RAMSES radiometer, the data size is approximately six times that of the OCR-504. Together with the moderately higher power consumption (45 mA compared to 25 mA for the OCR-504), this constrains either the measurement frequency or deployment duration of an Argo float equipped with this sensor. Therefore, reducing power consumption of the sensor and the dimension of the data onboard the platform prior to transmission could be important future steps. This process would probably demand embedded computing power in the sensor and the platform itself, which poses challenges on the commercially available instrumentation.

CONCLUSION

This review captures the current state of light field measurements onboard Argo floats, describes their application in bio-optical ocean studies, and points to future directions in the transition from multispectral toward hyperspectral radiometry. This transition would allow an exploitation of light field measurements far beyond to what is covered to date.

Moving forward in operating Argo radiometry, hyperspectral observations would provide more detailed insights through direct hyperspectral investigation of the depth-resolved light distribution in different waters bodies and would be relevant to ocean color products. The development of novel approaches that exploit this information will open new avenues for bio-optical long-term studies of global ocean change and foster its relevance for carbon cycle investigation by addressing phytoplankton not only in terms of biomass, but also with respect to taxonomic composition. Critically, exploiting these advantages requires the development, in parallel, of new algorithms and procedures for quality assessment, data management, and on-board data reduction, all of which are intrinsically related to the technical features of both sensor and platform.

AUTHOR CONTRIBUTIONS

AJ made the draft version. JW and OZ participated on the outline of the manuscript. All authors contributed to manuscript revisions and agreed to the submitted version.

FUNDING

This work is part of the Spectral Argo-N project funded by the German Federal Ministry of Education and Research (Grant No. 03V01478).

ACKNOWLEDGMENTS

The authors would like to thank the reviewers of this manuscript who helped to improve its quality by their constructive comments and suggestions.

REFERENCES

Ardyna, M., Lacour, L., Sergi, S., d'Ovidio, F., Sallée, J.-B., Rembauville, M., et al. (2019). Hydrothermal vents trigger massive phytoplankton blooms in the Southern Ocean. *Nat. Commun.* 10:2451. doi: 10.1038/s41467-019-09973-6

Argo Data Management Team (2021). *Argo User's Manual V3.4*. Brest: Ifremer.

Austin, R. W., and Petzold, T. J. (1981). "The determination of the diffuse attenuation coefficient of sea water using the Coastal Zone Color Scanner," in *Oceanography from Space*, ed. J. F. R. Gower (Boston, MA: Springer), 239–256. doi: 10.1007/978-1-4613-3315-9_29

Barbieux, M., Uitz, J., Gentili, B., de Fommervault, O. P., Mignot, A., Poteau, A., et al. (2019). Bio-optical characterization of subsurface chlorophyll maxima in the Mediterranean Sea from a biogeochemical-argo float database. *Biogeosciences* 16, 1321–1342. doi: 10.5194/bg-16-1321-2019

Barnard, A., Van Dommelen, R., Boss, E., Plache, B., Simontov, V., Orrico, C., et al. (2018). *A New Paradigm for Ocean Color Satellite Calibration and Validation: Accurate measurements of Hyperspectral Water Leaving Radiance from Autonomous Profiling Floats (HYPERNAV)*. Washington, DC: ESSOAr. doi: 10.1002/essoar.10500047.1

Biogeochemical-Argo Planning Group (2016). *The Scientific Rationale, Design and Implementation 21 Plan for a Biogeochemical-Argo Float Array*. Brest: Ifremer.

Bittig, H. C., Maurer, T. L., Plant, J. N., Wong, A. P. S., Schmechtig, C., Claustre, H., et al. (2019). A BGC-Argo guide: planning, deployment, data handling and usage. *Front. Mar. Sci.* 6:502. doi: 10.3389/fmars.2019.00502

Bracher, A., Bouman, H. A., Brewin, R. J. W., Bricaud, A., Brotas, V., Ciotti, A. M., et al. (2017). Obtaining phytoplankton diversity from ocean color: a scientific roadmap for future development. *Front. Mar. Sci.* 4:55. doi: 10.3389/fmars.2017.00055

Brewin, R. J. W., Dall'Olmo, G., Pardo, S., van Dongen-Vogels, V., and Boss, E. S. (2016). Underway spectrophotometry along the Atlantic Meridional Transect reveals high performance in satellite chlorophyll retrievals. *Remote Sens. Environ.* 183, 82–97. doi: 10.1016/j.rse.2016.05.005

Brown, C. A., Huot, Y., Purcell, M. J., Cullen, J. J., and Lewis, M. R. (2004). Mapping coastal optical and biogeochemical variability using an autonomous underwater vehicle and a new bio-optical inversion algorithm. *Limnol. Oceanogr. Methods* 2, 262–281. doi: 10.4319/lom.2004.2.262

Carder, K. L., Chen, F. R., Lee, Z. P., Hawes, S. K., and Kamykowski, D. (1999). Semianalytic moderate-resolution imaging spectrometer algorithms for chlorophyll a and absorption with bio-optical domains based on nitrate-depletion temperatures. *J. Geophys. Res. Oceans* 104, 5403–5421. doi: 10.1029/1998JC900082

Chai, F., Johnson, K. S., Claustre, H., Xing, X., Wang, Y., Boss, E., et al. (2020). Monitoring ocean biogeochemistry with autonomous platforms. *Nat. Rev. Earth Environ.* 1, 315–326. doi: 10.1038/s43017-020-0053-y

Chang, G., Mahoney, K., Briggs-Whitmire, A., Kohler, D., Mobley, C., Lewis, M., et al. (2004). The new age of hyperspectral oceanography. *Oceanography* 17:16. doi: 10.5670/oceanog.2004.43

Claustre, H., Johnson, K. S., and Takeshita, Y. (2020). Observing the global ocean with biogeochemical-Argo. *Ann. Rev. Mar. Sci.* 12, 23–48. doi: 10.1146/annurev-marine-010419-010956

Dierssen, H., Bracher, A., Brando, V., Loisel, H., and Ruddick, K. (2020). Data needs for hyperspectral detection of algal diversity across the globe. *Oceanography* 33, 74–79. doi: 10.5670/oceanog.2020.111

Doxaran, D., Lamquin, N., Park, Y.-J., Mazeran, C., Ryu, J.-H., Wang, M., et al. (2014). Retrieval of the seawater reflectance for suspended solids monitoring in the East China Sea using MODIS, MERIS and GOCI satellite data. *Remote Sens. Environ.* 146, 36–48. doi: 10.1016/j.rse.2013.06.020

Gerbi, G. P., Boss, E., Werdell, P. J., Proctor, C. W., Haëntjens, N., Lewis, M. R., et al. (2016). Validation of ocean color remote sensing reflectance using autonomous floats. *J. Atmos. Ocean. Technol.* 33, 2331–2352. doi: 10.1175/JTECH-D-16-0067.1

Gordon, H. R., and Morel, A. Y. (1983). *Remote Assessment of Ocean Color for Interpretation of Satellite Visible Imagery; a Review*. New York, NY: Springer-Verlag. doi: 10.1029/LN004

Gordon, H. R., and Clark, D. K. (1981). Clear water radiances for atmospheric correction of coastal zone color scanner imagery. *Appl. Opt.* 20, 4175–4180. doi: 10.1364/AO.20.004175

Gordon, H. R., Lewis, M. R., McLean, S. D., Twardowski, M. S., Freeman, S. A., Voss, K. J., et al. (2009). Spectra of particulate backscattering in natural waters. *Opt. Express* 17, 16192–16208. doi: 10.1364/OE.17.016192

Gregg, W. W., and Carder, K. L. (1990). A simple spectral solar irradiance model for cloudless maritime atmospheres. *Limnol. Oceanogr.* 35, 1657–1675. doi: 10.4319/lo.1990.35.8.1657

Gregg, W. W., and Rousseaux, C. S. (2017). Simulating PACE global ocean radiances. *Front. Mar. Sci.* 4:60. doi: 10.3389/fmars.2017.00060

Guanter, L., Kaufmann, H., Segl, K., Foerster, S., Rogass, C., Chabrillat, S., et al. (2015). The EnMAP spaceborne imaging spectroscopy mission for earth observation. *Remote Sens.* 7, 8830–8857. doi: 10.3390/rs70708830

IOCCG (2011). *Bio-Optical Sensors on Argo Floats: Reports of the International Ocean-Colour Coordinating Group, No. 11*, ed. H. Claustre (Dartmouth, NS: International Ocean-Colour Coordinating Group (IOCCG)), 89.

IOCCG (2013). *In-flight Calibration of Satellite Ocean-Colour Sensors: Reports of the International Ocean-Colour Coordinating Group, No. 14*, ed. R. Frouin (Dartmouth, NS: International Ocean-Colour Coordinating Group (IOCCG)), 106.

Isada, T., Hirawake, T., Kobayashi, T., Nosaka, Y., Natsuike, M., Imai, I., et al. (2015). Hyperspectral optical discrimination of phytoplankton community structure in Funka Bay and its implications for ocean color remote sensing of diatoms. *Remote Sens. Environ.* 159, 134–151. doi: 10.1016/j.rse.2014.12.006

Jochens, A. E., Malone, T. C., Stumpf, R. P., Hickey, B. M., Carter, M., Morrison, R., et al. (2010). Integrated ocean observing system in support of forecasting harmful algal blooms. *Mar. Technol. Soc. J.* 44, 99–121. doi: 10.4031/MTSJ.44.6.16

Kirk, J. T. O. (2011). *Light and Photosynthesis in Aquatic Ecosystems*, 3rd Edn. Cambridge: Cambridge University Press.

Kubryakov, A. A., Zatsepin, A. G., and Stanichny, S. V. (2019). Anomalous summer-autumn phytoplankton bloom in 2015 in the Black Sea caused by several strong wind events. *J. Mar. Syst.* 194, 11–24. doi: 10.1016/j.jmarsys.2019.02.004

Kutser, T. (2009). Passive optical remote sensing of cyanobacteria and other intense phytoplankton blooms in coastal and inland waters. *Int. J. Remote Sens.* 30, 4401–4425. doi: 10.1080/01431160802562305

Lacour, L., Ardyna, M., Stec, K. F., Claustre, H., Prieur, L., Poteau, A., et al. (2017). Unexpected winter phytoplankton blooms in the North Atlantic subpolar gyre. *Nat. Geosci.* 10, 836–839. doi: 10.1038/ngeo3035

Lacour, L., Briggs, N., Claustre, H., Ardyna, M., and Dall'Olmo, G. (2019). The intraseasonal dynamics of the mixed layer pump in the subpolar North Atlantic Ocean: a biogeochemical-argo float approach. *Glob. Biogeochem. Cycles* 33, 266–281. doi: 10.1029/2018GB005997

Lazzari, P., Salon, S., Terzić, E., Gregg, W. W., D'Ortenzio, F., Vellucci, V., et al. (2021). Assessment of the spectral downward irradiance at the surface of the Mediterranean Sea using the radiative Ocean-Atmosphere Spectral Irradiance Model (OASIM). *Ocean Sci.* 17, 675–697. doi: 10.5194/os-17-675-2021

Lee, Z., Carder, K. L., Steward, R. G., Peacock, T. G., Davis, C. O., and Patch, J. S. (1998). An empirical algorithm for light absorption by ocean water based on color. *J. Geophys. Res. Oceans* 103, 27967–27978. doi: 10.1029/98JC01946

Lee, Z., Du, K., and Arnone, R. (2005). A model for the diffuse attenuation coefficient of downwelling irradiance. *J. Geophys. Res.* 110:C02016. doi: 10.1029/2004JC002275

Leymarie, E., Penkerc'h, C., Vellucci, V., Lerebourg, C., Antoine, D., Boss, E., et al. (2018). ProVal: a new autonomous profiling float for high quality radiometric measurements. *Front. Mar. Sci.* 5:437. doi: 10.3389/fmars.2018.00437

Loizzo, R., Guarini, R., Longo, F., Scopa, T., Formaro, R., Facchinetti, C., et al. (2018). "Prisma: the Italian hyperspectral mission," in *Proceedings of the IGARSS 2018-2018 IEEE International Geoscience and Remote Sensing Symposium*, Valencia, 175–178. doi: 10.1109/IGARSS.2018.8518512

Maritorena, S., d'Andon, O. H. F., Mangin, A., and Siegel, D. A. (2010). Merged satellite ocean color data products using a bio-optical model: characteristics, benefits and issues. *Remote Sens. Environ.* 114, 1791–1804. doi: 10.1016/j.rse.2010.04.002

Maritorena, S., and Siegel, D. A. (2005). Consistent merging of satellite ocean color data sets using a bio-optical model. *Remote Sens. Environ.* 94, 429–440. doi: 10.1016/j.rse.2004.08.014

Maritorena, S., Siegel, D. A., and Peterson, A. R. (2002). Optimization of a semianalytical ocean color model for global-scale applications. *Appl. Opt.* 41, 2705–2714. doi: 10.1364/AO.41.002705

Mayot, N., d'Ortenzio, F., Taillandier, V., Prieur, L., De Fommervault, O. P., Claustre, H., et al. (2017). Physical and biogeochemical controls of the phytoplankton blooms in North Western Mediterranean Sea: a multiplatform approach over a complete annual cycle (2012–2013 DEWEX experiment). *J. Geophys. Res. Oceans* 122, 9999–10019. doi: 10.1002/2016JC012052

McClain, C. R., and Meister, G. (2012). *Mission Requirements for Future Ocean-Colour Sensors*. Dartmouth, NS: International Ocean Colour Coordinating Group (IOCCG).

Mignot, A., Ferrari, R., and Claustre, H. (2018). Floats with bio-optical sensors reveal what processes trigger the North Atlantic bloom. *Nat. Commun.* 9:190. doi: 10.1038/s41467-018-04181-0

Mignot, A., Claustre, H., Uitz, J., Poteau, A., d'Ortenzio, F., and Xing, X. (2014). Understanding the seasonal dynamics of phytoplankton biomass and the deep chlorophyll maximum in oligotrophic environments: a Bio-Argo float investigation. *Glob. Biogeochem. Cycles* 28, 856–876. doi: 10.1002/2013GB004781

Mobley, C. D. (1994). *Light and Water: Radiative Transfer in Natural Waters*. Cambridge, MA: Academic press.

Mobley, C. D., and Sundman, L. K. (2008). *Hydrolight 5 Ecolight 5*. Bellevue, WA: Sequoia Scientific Inc.

Morel, A., and Gentili, B. (1996). Diffuse reflectance of oceanic waters. III. Implication of bidirectionality for the remote-sensing problem. *Appl. Opt.* 35, 4850–4862. doi: 10.1364/AO.35.004850

Mueller, J. L., and Austin, R. W. (1992). *Ocean Optics Protocols for SeaWiFS Validation*. Greenbelt, MD: National Aeronautics and Space Administration, Goddard Space Flight Center.

Mueller, J. L., and Fargion, G. S. (2002). *Ocean Optics Protocols for Satellite Ocean Color Sensor Validation, Revision 3*, Vol. 210004. Greenbelt, MD: National Aeronautics and Space Administration, Goddard Space Flight Center.

Mueller, J. L., Morel, A., Frouin, R., Davis, C., Arnone, R., Carder, K., et al. (2003). *Ocean Optics Protocols for Satellite Ocean Color Sensor Validation, Revision 4: Radiometric Measurements and Data Analysis Protocols. NASA/TM-2003-21621/Rev-Vol III*, Vol. III. Greenbelt, MD: National Aeronautics and Space Administration, Goddard Space Flight Center, 78.

O'Reilly, J. E., Maritorena, S., Mitchell, B. G., Siegel, D. A., Carder, K. L., Garver, S. A., et al. (1998). Ocean color chlorophyll algorithms for SeaWiFS. *J. Geophys. Res. Oceans* 103, 24937–24953. doi: 10.1029/98JC02160

Organelli, E., Barbieux, M., Claustre, H., Schmechtig, C., Poteau, A., Bricaud, A., et al. (2017a). Two databases derived from BGC-Argo float measurements for marine biogeochemical and bio-optical applications. *Earth Syst. Sci. Data* 9, 861–880. doi: 10.5194/essd-9-861-2017

Organelli, E., and Claustre, H. (2019). Small phytoplankton shapes colored dissolved organic matter dynamics in the North Atlantic subtropical gyre. *Geophys. Res. Lett.* 46, 12183–12191. doi: 10.1029/2019GL084699

Organelli, E., Claustre, H., Bricaud, A., Barbieux, M., Uitz, J., D'Ortenzio, F., et al. (2017b). Bio-optical anomalies in the world's oceans: an investigation on the diffuse attenuation coefficients for downward irradiance derived from biogeochemical argo float measurements. *J. Geophys. Res. Oceans* 122, 3543–3564. doi: 10.1002/2016JC012629

Organelli, E., Claustre, H., Bricaud, A., Schmechtig, C., Poteau, A., Xing, X., et al. (2016). A novel near-real-time quality-control procedure for radiometric profiles measured by bio-argo floats: protocols and performances. *J. Atmos. Ocean. Technol.* 33, 937–951. doi: 10.1175/JTECH-D-15-0193.1

Poteau, A., Organelli, E., Boss, E., and Xing, X. (2019). *Quality Control for BGC-Argo Radiometry*. Brest: Ifremer.

Randelhoff, A., Lacour, L., Marec, C., Leymarie, E., Lagunas, J., Xing, X., et al. (2020). Arctic mid-winter phytoplankton growth revealed by autonomous profilers. *Sci. Adv.* 6:eabc2678. doi: 10.1126/sciadv.abc2678

Rehm, E., and McCormick, N. J. (2011). Inherent optical property estimation in deep waters. *Opt. Express* 19, 24986–25005. doi: 10.1364/OE.19.024986

Rehm, E., and Mobley, C. D. (2013). Estimation of hyperspectral inherent optical properties from in-water radiometry: error analysis and application to in situ data. *Appl. Opt.* 52, 795–817. doi: 10.1364/AO.52.000795

Ricour, F., Capet, A., D'Ortenzio, F., Delille, B., and Grégoire, M. (2021). Dynamics of the deep chlorophyll maximum in the black sea as depicted by BGC-Argo FLOATS. *Biogeosciences* 18, 755–774. doi: 10.5194/bg-18-755-2021

Riser, S. C., Freeland, H. J., Roemmich, D., Wijffels, S., Troisi, A., Belbéoch, M., et al. (2016). Fifteen years of ocean observations with the global Argo array. *Nat. Climate Change* 6, 145–153. doi: 10.1038/nclimate2872

Roemmich, D. (2001). "Argo: the Global array of profiling floats," in *Observing the Oceans in the 21st Century, Bureau of Meteorology*, eds C. J. Koblinsky and N. R. Smith (Melbourne, VC: GODAE Project Office, Bureau of Meteorology), 248–258.

SATLANTIC (2013). *Operation Manual for the OCR-504.SATLANTIC Operation Manual SAT-DN-00034, Revision G*. Halifax, NS: Satlantic, 66.

Schmechtig, C., Poteau, A., Claustre, H., and D'ortenzio, F. (2017). *Processing BGC-Argo Radiometric data at the DAC level. Version 1.1*. Villefranche-sur-Mer: IFREMER for Argo Data Management.

Schmid, C., Molinari, R. L., Sabina, R., Daneshzadeh, Y.-H., Xia, X., Forteza, E., et al. (2007). The real-time data management system for Argo profiling float observations. *J. Atmos. Ocean. Technol.* 24, 1608–1628. doi: 10.1175/JTECH2070.1

Seegers, B. N., Stumpf, R. P., Schaeffer, B. A., Loftin, K. A., and Werdell, P. J. (2018). Performance metrics for the assessment of satellite data products: an ocean color case study. *Opt. Express* 26, 7404–7422. doi: 10.1364/OE.26.007404

Sellner, K. G., Doucette, G. J., and Kirkpatrick, G. J. (2003). Harmful algal blooms: causes, impacts and detection. *J. Industr. Microbiol. Biotechnol.* 30, 383–406. doi: 10.1007/s10295-003-0074-9

Shen, L., Xu, H., and Guo, X. (2012). Satellite remote sensing of harmful algal blooms (HABs) and a potential synthesized framework. *Sensors* 12, 7778–7803. doi: 10.3390/s120607778

Stramska, M., Stramski, D., Hapter, R., Kaczmarek, S., and Stoñ, J. (2003). Bio-optical relationships and ocean color algorithms for the north polar region of the Atlantic. *J. Geophys. Res. Oceans* 108, 3143. doi: 10.1029/2001JC001195

Terzić, E., Lazzari, P., Organelli, E., Solidoro, C., Salon, S., D'Ortenzio, F., et al. (2019). Merging bio-optical data from Biogeochemical-Argo floats and models in marine biogeochemistry. *Biogeosciences* 16, 2527–2542. doi: 10.5194/bg-16-2527-2019

Trios (2021). *Ramses*. Rastede: TriOS Mess- und Datentechnik GmbH. Available online at: www.trios.de (accessed May 20, 2021).

Werdell, P. J., and Bailey, S. W. (2005). An improved in-situ bio-optical data set for ocean color algorithm development and satellite data product validation. *Remote Sens. Environ.* 98, 122–140. doi: 10.1016/j.rse.2005.07.001

Werdell, P. J., McKinna, L. I. W., Boss, E., Ackleson, S. G., Craig, S. E., Gregg, W. W., et al. (2018). An overview of approaches and challenges for retrieving marine inherent optical properties from ocean color remote sensing. *Progr. Oceanogr.* 160, 186–212. doi: 10.1016/j.pocean.2018.01.001

Werdell, P. J., Proctor, C. W., Boss, E., Leeuw, T., and Ouhssain, M. (2013). Underway sampling of marine inherent optical properties on the Tara Oceans expedition as a novel resource for ocean color satellite data product validation. *Methods Oceanogr.* 7, 40–51. doi: 10.1016/j.mio.2013.09.001

Wojtasiewicz, B., Hardman-Mountford, N. J., Antoine, D., Dufois, F., Slawinski, D., and Trull, T. W. (2018). Use of bio-optical profiling float data in validation of ocean colour satellite products in a remote ocean region. *Remote Sens. Environ.* 209, 275–290. doi: 10.1016/j.rse.2018.02.057

Wolanin, A., Soppa, M. A., and Bracher, A. (2016). Investigation of spectral band requirements for improving retrievals of phytoplankton functional types. *Remote Sens.* 8:871. doi: 10.3390/rs8100871

Wollschläger, J., Tietjen, B., Voß, D., and Zielinski, O. (2020). An empirically derived trimodal parameterization of underwater light in complex coastal waters–A case study in the North Sea. *Front. Mar. Sci.* 7:512. doi: 10.3389/fmars.2020.00512

Wong, A., Keeley, R., and Carval, T. (2020). *Argo Quality Control Manual for CTD and Trajectory Data*. Brest: Ifremer.

Xi, H., Hieronymi, M., Röttgers, R., Krasemann, H., and Qiu, Z. (2015). Hyperspectral differentiation of phytoplankton taxonomic groups: a comparison between using remote sensing reflectance and absorption spectra. *Remote Sens.* 7, 14781–14805. doi: 10.3390/rs71114781

Xing, X., Boss, E., Zhang, J., and Chai, F. (2020). Evaluation of ocean color remote sensing algorithms for diffuse attenuation coefficients and optical depths with data collected on BGC-Argo floats. *Remote Sens.* 12:2367. doi: 10.3390/rs12152367

Xing, X., Briggs, N., Boss, E., and Claustre, H. (2018). Improved correction for non-photochemical quenching of in situ chlorophyll fluorescence based on a synchronous irradiance profile. *Opt. Express* 26, 24734–24751. doi: 10.1364/OE.26.024734

Xing, X., Claustre, H., Uitz, J., Mignot, A., Poteau, A., and Wang, H. (2014). Seasonal variations of bio-optical properties and their interrelationships observed by Bio-Argo floats in the subpolar North A tlantic. *J. Geophys. Res. Oceans* 119, 7372–7388. doi: 10.1002/2014JC010189

Xing, X., Morel, A., Claustre, H., Antoine, D., D'Ortenzio, F., Poteau, A., et al. (2011). Combined processing and mutual interpretation of radiometry and fluorimetry from autonomous profiling Bio-Argo floats: chlorophyll a retrieval. *J. Geophys. Res. Oceans* 116:C0602. doi: 10.1029/2010JC006899

Xing, X., Morel, A., Claustre, H., d'Ortenzio, F., and Poteau, A. (2012). Combined processing and mutual interpretation of radiometry and fluorometry from autonomous profiling Bio-Argo floats: 2. Colored dissolved organic matter absorption retrieval. *J. Geophys. Res. Oceans* 117:C04022. doi: 10.1029/2011JC007632

Zibordi, G., and Voss, K. J. (2014). In situ optical radiometry in the visible and near infrared. *Exp. Methods Phys. Sci.* 47, 247–304. doi: 10.1016/B978-0-12-417011-7.00010-6

Zielinski, O., Busch, J. A., Cembella, A. D., Daly, K. L., Engelbrektsson, J., Hannides, A. K., et al. (2009). Detecting marine hazardous substances and organisms: sensors for pollutants, toxins, and pathogens. *Ocean Sci.* 5:329. doi: 10.5194/os-5-329-2009

Zielinski, O., Cembella, B., and Heuermann, R. (2006). "Bio-optical sensors onboard autonomous profiling floats," in *Proceedings of the 25th International Conference on Offshore Mechanics and Arctic Engineering*, Vol. 47462, Hamburg, 735–739. doi: 10.1115/OMAE2006-92482

Conflict of Interest: The authors declare that the research was conducted in the absence of any commercial or financial relationships that could be construed as a potential conflict of interest.

APPENDIX

APPENDIX A | Notations used in this review.

Symbol or abbreviation	Significance/units
L	Radiance (W $m^{-2}sr^{-1}nm^{-1}$)
L_u	Upwelling radiance (W $m^{-2}sr^{-1}nm^{-1}$)
E_d	Downward irradiance (W m^{-2} nm^{-1})
L_{wn} (λ)	Water-leaving radiance (W $m^{-2}sr^{-1}nm^{-1}$)
r_{rs} (λ)	Under-water surface remote sensing reflectance (sr^{-1})
R_{rs} (λ)	Above-water surface remote sensing reflectance (sr^{-1})
K_d (λ)	Diffuse attenuation coefficient at wavelength λ (m^{-1})
K_{bio} (λ)	Non-watery diffuse attenuation coefficient at wavelength λ (m^{-1})
K_{star} (λ)	Chlorophyll-specific attenuation coefficient at wavelength λ (units of square meters per milligram of chlorophyll)
PAR	Photosynthetically Available Radiation (μmole photons m^{-2} s^{-1})
K_d (*PAR*)	Diffuse attenuation coefficient of PAR (m^{-1})
chl-a	Chlorophyll-a concentration (mg m^{-3})
CDOM	Colored dissolved organic matter
Z_{eu}	Euphotic depth (m)
IOP	Inherent optical property
AOP	Apparent optical property